Relaxation Dynamics of Highly Vibrationally Excited Picoline Isomers (E_{vib} = 38 300 cm^{-1}) with CO_2: The Role of State Density in Impulsive Collisions†

Elisa M. Miller,‡ Liat Murat,‡ Nicholas Bennette,‡ Mitchell Hayes,‡ and Amy S. Mullin*,‡,§

Department of Chemistry, Metcalf Center for Science and Engineering, Boston University, Boston, Massachusetts 02215, and Department of Chemistry and Biochemistry, University of Maryland, College Park, Maryland 20472

Received: August 23, 2005; In Final Form: November 15, 2005

Strong collisions of highly vibrationally excited picoline isomers and CO_2 (00^00) were investigated using high resolution transient IR absorption probing to investigate the role of donor state density. Vibrationally excited 3-picoline and 4-picoline (3-methylpyridine and 4 methylpyridine) with E_{vib} = 38300 cm^{-1} were prepared by 266 nm excitation followed by rapid internal conversion. Transient IR probe measurements of the nascent rotational and translational energy gain in CO_2 (00^00) show that large ΔE collisions for 3- and 4-picoline are similar to those for excited 2-picoline. The probability distributions for the large ΔE energy transfer of the three isomers have similar dependence on ΔE. The results are compared with other earlier results demonstrating that the shape of the large ΔE probability distribution correlates with the ΔE dependence of the donor vibrational state density. The results are discussed in terms of the GRETCHEN model for collisional relaxation.

Introduction

Highly excited molecules are important species in many chemical reactions and the collisional relaxation of high energy molecules competes directly with unimolecular reactions and other activated processes.[1] State resolved IR experiments that probe energy in small bath molecules have identified both long- and short-range mechanisms for the collisional energy transfer that quenches vibrationally hot molecules.[2−4] Short-range impulsive interactions are one of the major mechanisms for relaxation wherein highly vibrationally excited donor molecules lose large amounts of energy (ΔE > 3000 cm^{-1}) of vibrational energy in single encounters with small polyatomic bath species, leaving the scattered molecules with increased amounts of rotational and translational energy.

Because transient IR probing experiments focus on energy gain in the small bath molecules, these studies are especially useful in providing detailed information about the strong collisions that make up the high energy tail of the energy transfer distribution function $P(\Delta E)$. Transient IR bath probing can be applied to any bath molecules with sufficient absorption intensity and an IR spectrum that is sparse enough to characterize the transient line shapes of individual IR transitions. In a complementary approach, Luther and co-workers have investigated the collisional relaxation of highly excited toluene and azulene using kinetically controlled selective ionization (KCSI).[5−8] In KCSI, the vibrationally excited donor molecules are monitored as they appear in lower energy windows following collisions with bath molecules and the distribution of transition probabilities $P(E',E)$ is obtained. This technique has proven very effective at characterizing both the low and high energy parts of the energy transfer distribution function and is readily applied to a variety of bath gases.

A number of theoretical and computational approaches have been taken to understand the collisional relaxation of highly excited molecules. In 1984, Gilbert[9] developed the "biased random walk" model which describes energy relaxation in terms of diffusion through the available energy space. In the Gilbert model, the shape of the distribution function is a shifted Gaussian which is not in good agreement with KCSI measurements. Early statistical approaches by Rabinovitch[10,11] and Troe[12−14] and their co-workers assumed that all degrees of freedom are equilibrated in the collision pair. This assumption overestimates the amount of energy transferred per collision. More recently, Nordholm and co-workers[15] have developed the partially ergodic collision theory (PECT) which allows partial equilibration of the collision pair and has successfully predicted the distribution function shapes for toluene and azulene that have been measured by Luther and co-workers.[5−8] In 1990, Lim and Gilbert[16] performed pioneering trajectory studies on azulene energy transfer and found that impulsive collisions led to large ΔE energy transfer events. Since then, the relaxation of a number of highly excited molecules has been simulated with both atomic and molecular collision partners.[7,17−30] These studies have shown that energy loss via strong collisions is common, although a range of mechanisms is responsible for the large ΔE collisions.

Earlier high resolution transient IR studies of energy transfer from vibrationally hot azabenzene molecules to CO_2 and H_2O bath molecules have shown that the distribution of strong collisions correlates with the energy dependence of the state density of the highly excited donor molecules.[31−33] These studies focused on collisions of a series of donor molecules of increasing complexity: pyrazine, pyridine, 2-methylpyridine (2-picoline), and 2,6-dimethylpyridine (2,6-lutidine). In each case the highly vibrationally excited donor molecules were prepared with $E_{vib} \sim$ 38500 cm^{-1} by electronic excitation at 266 nm followed by rapid radiationless decay. The nascent distributions of

† Part of the special issue "Jürgen Troe Festschrift".

* To whom correspondence should be addressed at the University of Maryland.

‡ Boston University.

§ University of Maryland, College Park, Maryland 20472.

10.1021/jp054762y CCC: $33.50
Published on Web 12/23/2005

rotational and translational energy gain in the CO_2 and H_2O bath molecules were probed by high resolution transient IR absorption. The observed correlation between the donor vibrational state density and the energy transfer distribution is intriguing both as an insight into what controls energy transfer from highly excited molecules and as a potential predictive tool of collisional relaxation efficiency.

In the previous studies, there were a number of potentially important properties that varied among the donor molecules, including molecular structure, polarity, and state density. In the work here, we target isomers with nearly identical properties to test the correlation of energy transfer with state density. We report on the large ΔE collisions of two picoline isomers, 3-picoline (E_{vib}) and 4-picoline (E_{vib}), with CO_2 and compare their energy loss distributions with earlier results for quenching of 2-picoline (E_{vib}).[33] The frequencies of the 36 vibrational modes change little from isomer to isomer and thus the vibrational state density of each isomer is nearly identical. The location of the methyl group changes the electronic distribution of the molecule, and the polarity decreases somewhat as the methyl group is moved away from the nitrogen lone pair with μ(2-picoline) = 2.76 D, μ(3-picoline) = 2.4 D, and μ(4-picoline) = 1.85 D. This series of hot donors provides the opportunity to compare relaxation behavior in different highly excited molecules while features such as energy, mass, number of modes, mode frequencies, and state density remain essentially constant.

Experimental Section

The studies described here were performed using a transient IR diode laser spectrometer, which has been described previously.[34] A 1:1 mixture of gas phase donor and CO_2 molecules was introduced to a 300 cm flowing-gas collision cell at a total pressure of ~20 mTorr. The excitation of the donor was accomplished by absorption of 266 nm pulsed light from the fourth harmonic of a Nd:YAG laser (Continuum series 8010). The UV intensity was kept below 2.1 MW/cm^2 and typically the concentration of picoline (E_{vib} = 38300 cm^{-1}) was ~7% of the total picoline concentration. Energy gain into individual rotational states of CO_2 (00^00) resulting from collisions with hot picoline was monitored by transient absorption of IR light at λ = 4.3 μm from a liquid nitrogen cooled CW diode laser (Laser Photonics L5736). After passing through the collision cell and a monochromator, the transmitted intensity of the IR light was collected using a liquid nitrogen cooled InSb detector (Judson Technologies J10DM204 R01 M-30) and amplifier with 100 ns response time and stored using a digital oscilloscope (LeCroy 9304A). The fractional absorption $\Delta I/I_0$ was collected as a function of time after each UV laser pulse using a dual channel technique. Typically transient measurements of rotational populations were averaged over ~200 UV laser pulses.

For all measurements, the output frequency of the IR laser was controlled using active feedback stabilization with ~8% of the laser output. For rotational populations, the diode laser current was locked to the top of the rovibrational probe transition using a static CO_2 reference cell. Population measurements for the J = 62−80 states of CO_2 (00^00) were collected relative to the J = 66 state to minimize error due to long-term fluctuations in cell pressure and laser power. Translational energy gain measurements were obtained by collecting Doppler-broadened line shapes for individual states of CO_2. For these measurements, the output of the IR laser was locked to a fringe of a scanning Fabry−Perot Etalon that was tuned ~0.03 cm^{-1} over an individual CO_2 transition. Transient absorption was collected at ~40 discrete frequencies to map out the nascent Doppler-broadened line shape.

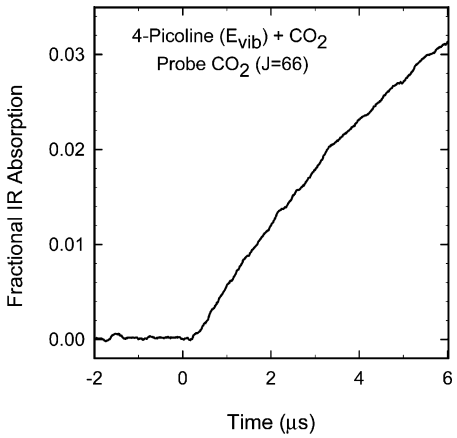

Figure 1. Transient IR absorption for appearance of CO_2 (00^00) in the J = 66 state from collisions with vibrationally excited 3-picoline. The 266 nm UV laser is fired at t = 0 to prepare vibrationally excited 3-picoline (or 4-picoline) with E_{vib} = 38330 cm^{-1}. CO_2 populations at t = 1 μs result primarily from single collisions of CO_2 with vibrationally excited donors at a total cell pressure near 20 mTorr.

The 3-picoline (C_6H_7N, Aldrich 99.5+ % purity) and 4-picoline (C_6H_7N, Avocado Research Chemicals Ltd. 98% purity) were purified with three freeze−pump−thaw cycles prior to use. Research Grade CO_2 (Matheson, 99.995% purity) was used for energy transfer measurements with no further purification. For the reference cell, CO_2 (Northeast Airgas, 99.8% purity) was used without further purification.

Results and Discussion

(1) CO_2 Rotational Energy Gain from 3-Picoline (E_{vib}) and 4-Picoline (E_{vib}). Rotational energy gain in CO_2 resulting from collisions with highly vibrationally excited 3-picoline and 4-picoline was measured for CO_2 (00^00) molecules with J = 62−80. Figure 1 shows the transient IR signals for CO_2 (00^00) in the J = 66 state resulting from collisions with vibrationally excited 3-picoline and 4-picoline. At t = 0, the 266 nm pulse generates highly vibrationally excited donor molecules and subsequent collisions remove donor vibrational energy. The fractional IR absorption signal in Figure 1 corresponds to population increases in the J = 66 state of CO_2 (00^00) as a function of time. The average time between collisions is ~4 μs, and population measurements taken at 1 μs correspond essentially to energy transfer from single collisions.

Nascent populations of individual rotational states of CO_2 (00^00) were determined using the fractional absorption at t = 1 μs and the CO_2 absorption coefficients from the HITRAN database.[35] Figure 2 shows the Boltzmann plot of the nascent CO_2 rotational states J ~ 62−80 that result from collisions with 3- and 4-picoline along with earlier results for 2-picoline.[33] The rotational populations include contributions from the transient Doppler-broadened line widths that are presented in the next section. The distribution of CO_2 rotational states from 3-picoline quenching is T_{rot} = 581 ± 55 K. For 4-picoline, the CO_2 distribution is T_{rot} = 619 ± 60 K. For comparison, the CO_2 distribution that results from quenching 2-picoline is T_{rot} = 616 ± 60 K. The results for the three isomers agree within experimental error.

(2) CO_2 Translational Energy Gain from 3-Picoline (E_{vib}) and 4-Picoline (E_{vib}). The translational energy that is released in the collisional quenching of highly vibrationally excited picoline isomers by CO_2 was determined by measuring Doppler-

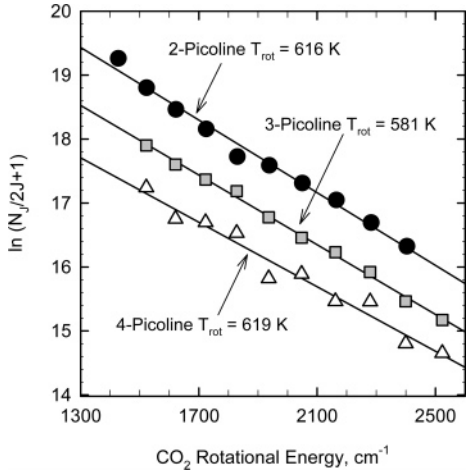

Figure 2. Nascent rotational distributions of the $J = 62-80$ states of CO_2 (00^00) after collisions with 3-picoline (E_{vib}) and 4-picoline (E_{vib}) and for $J = 60-78$ after collisions with 2-picoline (E_{vib}). The CO_2 populations were determined $t = 1$ μs following UV excitation of the hot donors.

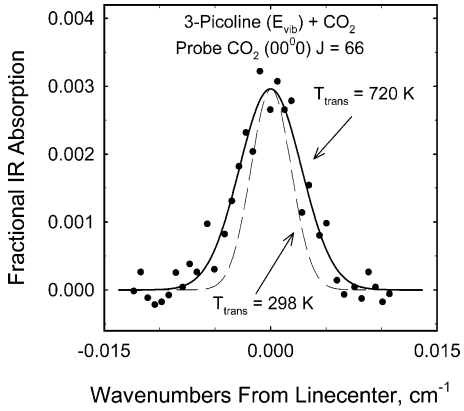

Figure 3. Nascent Doppler-broadened line profile for the $J = 66$ state of CO_2 (00^00) following collisions with highly excited 3-picoline (E_{vib}). The data are collected at $t = 1$ μs following excitation of the 3-picoline and are fit to a Gaussian distribution (solid line). The dashed line shows the line shape at 298 K.

broadened transient line shapes for a number of CO_2 IR transitions at $t = 1$ μs following the UV pulse. Figure 3 shows the 1 μs population data for CO_2 $J = 66$ as a function of IR frequency following collisions with 3-picoline. Fitting the data in Figure 3 to a Gaussian line shape (solid line) yields a full width half-maximum (fwhm) line width of $\Delta\nu_{obs} = 0.0066 \pm 0.0009$ cm^{-1}. The transient line shape is broadened relative to the line shape at 298 K, as shown in Figure 3 by the dashed line. Figure 4 shows the transient line shape for CO_2 $J = 66$ following collisions with 4-picoline, where the fwhm is $\Delta\nu_{obs} = 0.0069 \pm 0.0009$ cm^{-1}. The fwhm for each J state from $J = 62$ to $J = 80$ was measured for 3-picoline quenching and the results are shown in Table 1. Line shapes were measured for a representative sample of CO_2 states that are populated in quenching 4-picoline and the results are shown in Table 1. Translational temperatures for CO_2 that result from collisions with 3- and 4-picoline were determined from the measured line widths and are shown in Figure 5, along with previous results for 2-picoline. A comparison of the line width data for 3-picoline and 4-picoline quenching in CO_2 shows similar results for both donors, both in the magnitude of the broadening and in the dependence on CO_2 rotational quantum number. The increase in translational energy as a function of bath rotational energy is indicative of an impulsive energy transfer mechanism.

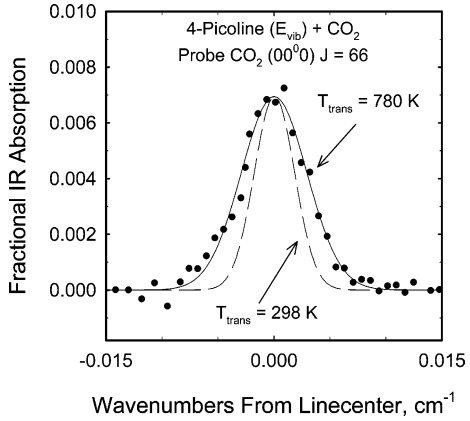

Figure 4. Nascent Doppler-broadened line profile for the $J = 66$ state of CO_2 (00^00) following collisions with highly excited 4-picoline (E_{vib}). The data are collected at $t = 1$ μs following excitation of the 4-picoline and are fit to a Gaussian distribution (solid line). The dashed line shows the line shape at 298 K.

TABLE 1: Doppler-Broadened Line Widths for CO_2 (00^00, J) Following Collisions with Highly Excited 3-Picoline and 4-Picoline (E_{vib} = 38300 cm^{-1})

CO_2 (00°0,J)		3-picoline		4-picoline	
J	E_{rot}, cm^{-1}	$\Delta\nu_{obs}$, cm^{-1} [a]	T_{trans}, K (lab)[b]	$\Delta\nu_{obs}$, cm^{-1} [a]	T_{trans}, K (lab)[b]
62	1522.1611	0.0060	590 ± 200		
64	1621.0037	0.0063	660 ± 210		
66	1722.9413	0.0066	720 ± 220	0.0069	780 ± 230
68	1827.9724	0.0074	910 ± 240		
70	1936.0953	0.0075	930 ± 250	0.0073	880 ± 240
72	2047.3081	0.0078	1010 ± 260		
74	2162.6090	0.0080	1070 ± 270	0.0073	900 ± 240
76	2278.9962	0.0081	1100 ± 270		
78	2399.4677	0.0085	1210 ± 280	0.0081	1100 ± 270
80	2523.0216	0.0095	1510 ± 320		

[a] Full width half-maximum line widths $\Delta\nu_{obs}$ from fitting transient line shape data to a Gaussian function. Transient absorption lineprofiles of CO_2 (00^00, J) were collected at $t = 1$ μs following UV excitation of 3- and 4-picoline. Some CO_2 line width data for 4-picoline collisions were not collected due to multimode laser output. All line widths are reported to within ±0.0009 cm^{-1}. [b] Lab frame translational temperatures for CO_2 following collisions with highly excited 3- and 4-picoline, determined using $T_{trans}(K) = (mc^2/8k_B\ln 2)(\Delta\nu_{obs}\nu_0)^2$ where m is the mass of CO_2, k_B is Boltzmann's constant, c is the speed of light, and ν_0 is the rovibrational transition frequency.

Previous data for 2-picoline/CO_2 collisions are included in Figure 5 and show similar behavior.

(3) Rate constants for CO_2 Energy Gain from 3-Picoline (E_{vib}) and 4-Picoline (E_{vib}). Rate constants for energy gain into rotational states of CO_2 have been determined by measuring the appearance of population in individual CO_2 states as a function of time at known donor and bath concentrations. For short times following the UV pulse, the appearance of individual states of CO_2 results predominantly from collisions with vibrationally excited donor molecules and the bimolecular rate constant k_2^J for energy gain into an individual CO_2 rotational state was obtained using eq 1.

$$\frac{d[CO_2(00^00,J)]}{dt} = k_2^J[\text{donor}(E_{vib})][CO_2] \qquad (1)$$

The change of the CO_2 population in the J rotational state was determined by the increase in the transient IR absorption from $t = 0$ to 1 μs as shown in Figure 1. The population measurements include contributions from the observed Doppler-

TABLE 2: State-Specific Energy Transfer Rate Constants for Energy Gain in CO_2 Following Collisions with Highly Vibrationally Excited Picoline Isomers Picoline ($E_{vib} \sim 38\,330$ cm^{-1}) + CO_2 → Picoline ($E_{vib} - \Delta E$) + CO_2 (00^00, J)

CO_2 (00^00)		k_2^J, 10^{-13} cm^3 molecule^{-1} s^{-1}		
J	E_{rot}, cm^{-1}	2-picoline[a]	3-picoline	4-picoline
62	1522.1611	18 ± 6	10 ± 3	12 ± 4
64	1621.0037	14 ± 5	8.3 ± 2.8	10 ± 3
66	1722.9413	12 ± 4	6.7 ± 2.2	8.2 ± 2.7
68	1827.9724	9.3 ± 3.1	5.3 ± 1.8	6.8 ± 2.2
70	1936.0953	7.3 ± 2.4	4.1 ± 1.3	5.2 ± 1.7
72	2047.3081	5.8 ± 1.9	3.2 ± 1.1	4.2 ± 1.4
74	2161.6090	4.5 ± 1.5	2.5 ± 0.8	3.3 ± 1.1
76	2278.9962	3.5 ± 1.2	1.9 ± 0.6	2.6 ± 0.9
78	2399.4677	2.7 ± 0.9	1.5 ± 0.5	2.0 ± 0.7
80	2523.0216	2.5 ± 0.8	1.1 ± 0.3	1.6 ± 0.5
$k_2^{int} = \sum k_2^J Z^b$		$(7.9 \pm 2.6) \times 10^{-12}$	$(4.5 \pm 1.5) \times 10^{-12}$	$(5.6 \pm 1.9) \times 10^{-12}$

[a] Results for 2-picoline are taken from ref 33. [b] Units of k_2^{int} are cm^3 molecule^{-1} s^{-1}.

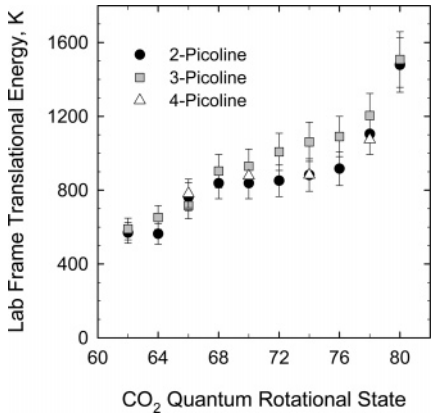

Figure 5. Lab frame kinetic energy of CO_2 following collisions with vibrationally excited picoline donors as a function of the CO_2 rotational energy. Data were collected at 1 μs following UV excitation. T_{trans} values were determined as described in Table 1.

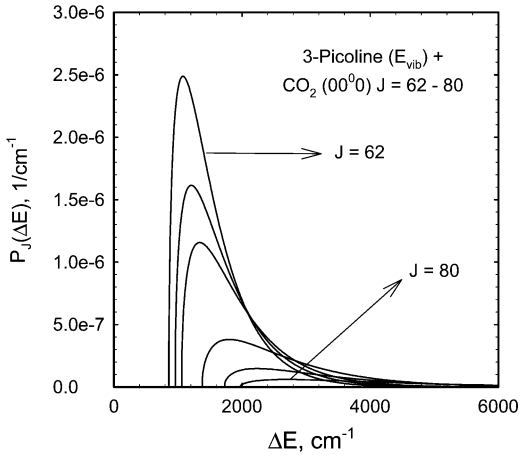

Figure 6. State-resolved probability distribution functions $P^J(\Delta E)$ for individual states of CO_2 (00^00) $J = 60-78$ that are populated by collisions with highly excited 3-picoline. The distribution functions are generated using nascent Doppler-broadened line width measurements and absolute rate constants.

broadened line widths measured at $t = 1$ μs. The energy gain rate constant for the $J = 66$ state of CO_2 following collisions with 3-picoline is $k_2^J = (6.7 \pm 2.2) \times 10^{-13}$ cm^3 molecule^{-1} s^{-1}. For 4-picoline quenching, the rate constant for the $J = 66$ state of CO_2 is similar to $k_2^J = (8.3 \pm 2.8) \times 10^{-13}$ cm^3 molecule^{-1} s^{-1}. Values for k_2^J values for quenching 3-picoline and 4-picoline with CO_2 are listed in Table 2 along with previous results for 2-picoline collisions. The rates for 3- and 4-picoline are identical to within our experimental uncertainty. The rates for 2-picoline quenching are slightly larger than those for the 3- and 4-isomers but are within experimental error of them. An integrated rate constant k_2^{int} is the summation of k_2^J values for $J = 62-80$ and is listed at the bottom of Table 2 for each picoline isomer.

(4) P(ΔE) Curves for Quenching of 3-Picoline and 4-Picoline. The high energy tails of the energy transfer distribution functions $P(\Delta E)$ for 3- and 4-picoline with CO_2 were obtained from the state resolved energy transfer data reported in this paper. The procedure for obtaining the distribution functions has been presented previously,[36] and the overall scheme is outlined here. The state resolved translational energy distribution data in Figure 5 determine the shape of the distribution function for ΔE (energy lost from hot picoline molecules) associated with energy gain in individual J states of CO_2. Several J-specific distribution functions $P^J(\Delta E)$ for 3-picoline quenching with CO_2 are shown in Figure 6. The origin of each $P^J(\Delta E)$ curve corresponds to the average change in CO_2 rotational energy associated with a specific final J state of CO_2. The shape of each $P^J(\Delta E)$ curve corresponds to the distribution of picoline vibrational energy that is converted to translational energy via collisions. The overall probability of each J-specific curve is established by ratio of the energy transfer rate constants listed in Table 2 to the collision rate constant. The J-specific curves are summed to give an overall $P(\Delta E)$ curve for the strong collisions of the vibrationally hot picoline isomers with CO_2. The high energy tail of the $P(\Delta E)$ curve for the collisional quenching of highly vibrationally excited 3-picoline with CO_2 is shown in Figure 7. The intensity of the $P(\Delta E)$ at $\Delta E = 4000$ cm^{-1} is $\sim 5 \times 10^{-6}$ per cm^{-1} which is comparable to KCSI results for azulene and toluene.[6,8] It should be noted that the distribution functions in Figures 6 and 7 do not include any contribution to energy gain into picoline rotation. Lack of information about picoline rotation introduces additional uncertainty in ΔE.

The upper panel of Figure 8 is a semilog plot of the $P(\Delta E)$ curves for the three picoline isomers for $\Delta E = 3000-10000$ cm^{-1}. Slight differences in the translational and rotational energy distributions for the picoline isomers account for the slight differences in the shape of the $P(\Delta E)$ functions but overall the shapes of the high energy components of the distribution functions for the isomers are quite similar. The lower panel of Figure 8 shows $P(\Delta E)$ data for quenching other highly vibrationally excited azabenzenes that have been reported previously.[33] The high energy tail of the distribution function for

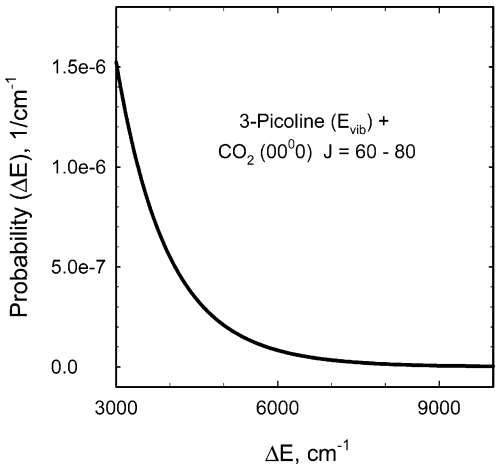

Figure 7. High energy tail of the probability distribution function for energy gain in CO_2 (00^00) $J = 60-78$ following collisions with highly excited 3-picoline obtained by summing state-resolved distributions.

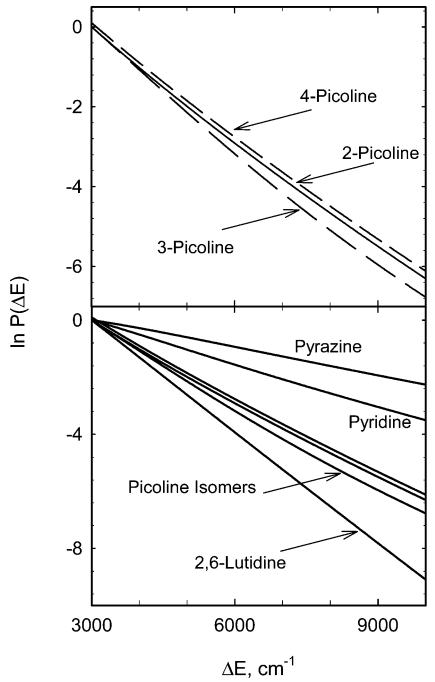

Figure 8. Semilog plot of the $P(\Delta E)$ distribution functions for energy transfer between the hot azabenzene donors and CO_2 for $\Delta E > 3000$ cm^{-1}. As the number of vibrational modes increases in the donor molecule, the exponential fitting parameter β_{obs} increases. Data for other azabenzenes are from ref 33.

each donor species in Figure 8 was fit to an exponential decay function given by eq 2.

$$P(\Delta E) = \alpha_{obs} \exp(-\beta_{obs}\Delta E) \qquad (2)$$

The shape parameter β_{obs} for each donor species is listed in Table 3.

Figure 8 and Table 3 illustrate several important points. The high energy tails of the energy transfer distribution functions for the picoline isomers are nearly indistinguishable and they are characterized by essentially the same values of β_{obs}. The large ΔE relaxation of these isomers with CO_2 occurs by an impulsive mechanism that is not particularly sensitive to differences in the donor dipole moment ($\Delta\mu \sim 1$D) when all other things are equal. Finally, the data presented here show that the slope of the high energy part of the $P(\Delta E)$ curves for different vibrationally hot donors increases monotonically with the number of vibrational modes in the molecule.

TABLE 3: Shape Parameters for the Observed Energy Transfer Distribution Functions (β_{obs}) the Energy Dependence of the State Density (β_ρ) for a Number of High Energy Donors with CO_2

donor molecule	E_{vib}, cm^{-1}	β_{obs}, $10^{-4}/cm^{-1}$ [a]	β_ρ, $10^{-4}/cm^{-1}$ [b]
pyrazine[c]	37950	3.3	5.08
pyridine[c]	37950	5.0	5.52
2-picoline[c]	38330	10	6.87
3-picoline[d]	38330	9.5	6.87
4-picoline[d]	38330	9.3	6.87
2,6-lutidine[c]	38740	13	8.07
hexafluorobenzene[e]	41822	7.5	5.7
toluene[f]	40000	7.8	6.7
azulene[g]	40000	10.3	7.8

[a] The shape parameter β_{obs} for large ΔE energy transfer is determined by fitting the high energy tail of the energy transfer distribution function to an exponential function (eq 2). [b] The shape parameter β_ρ for the vibrational state density of each donor molecules is determined by fitting the energy dependent state density to an exponential function (eq 3). [c] Data taken from ref 33. [d] This work. [e] β_{obs} taken from ref 38. [f] The value of β_{obs} is evaluated at $E_{vib} = 40\,000$ cm^{-1} based on coefficients given in ref 6 [g] Coefficients for β_{obs} taken from ref 8.

(5) Correlation of $P(\Delta E)$ with State Density. Previously, we reported that the shape of the high energy tail of $P(\Delta E)$ for quenching in CO_2 and H_2O baths correlated with the energy dependence of donor vibrational state density.[31−33] This observation is consistent with a golden rule treatment to describe the collisional quenching of highly vibrationally excited molecules known as GRETCHEN (golden rule excitation transfer in collisions of high energy molecules). Here we test this correlation for the picoline isomers. The vibrational state density for each picoline isomer was calculated as a function of internal energy by a direct sum of states using the Beyer−Swinehart algorithm[37] and harmonic vibrational frequencies. At an initial energy of $E_{vib} = 38330$ cm^{-1}, the vibrational state density of the picoline isomers is $\rho = 7 \times 10^{17}$ states/cm^{-1}. The energy dependent state densities $\rho(E - \Delta E)$ for 2-, 3-, and 4-picoline are shown in the top panel of Figure 9, along with state densities for pyrazine, pyridine, and 2,6-lutidine. The state density profiles for the picoline isomers are nearly indistinguishable due similarities in their vibrational frequencies. At an initial vibrational energy near 38000 cm^{-1} each species considered in Figure 9 has a near continuum of vibrational states with state densities of $\rho = 5 \times 10^{12}$ states per cm^{-1} for pyrazine and $\rho = 4 \times 10^{19}$ states per cm^{-1} for 2,6-lutidine. The state density for each species decreases as the internal energy decreases and eventually approaches values less than one as the internal energy approaches zero.

The lower panel of Figure 9 shows that the state density of the hot donors initially at $E = 38000$ cm^{-1} decays nearly exponentially as a function of internal energy for $\Delta E = 0$ to 12000 cm^{-1}, a range of ΔE that is applicable to the energy transfer measurements of Figure 8. Each of the state density curves in the lower panel of Figure 9 was fit to an exponential decay function given by eq 3.

$$\rho(E - \Delta E) = \alpha_\rho \exp(-\beta_\rho \Delta E) \qquad (3)$$

The resulting state density shape parameters β_ρ are listed in Table 3. The experimental shape parameter (β_{obs}) is compared in Figure 10 to the state density shape parameter (β_ρ) for each vibrationally hot donor we have measured (shown in open circles). The linear correlation of β_{obs} with β_ρ is clear in Figure

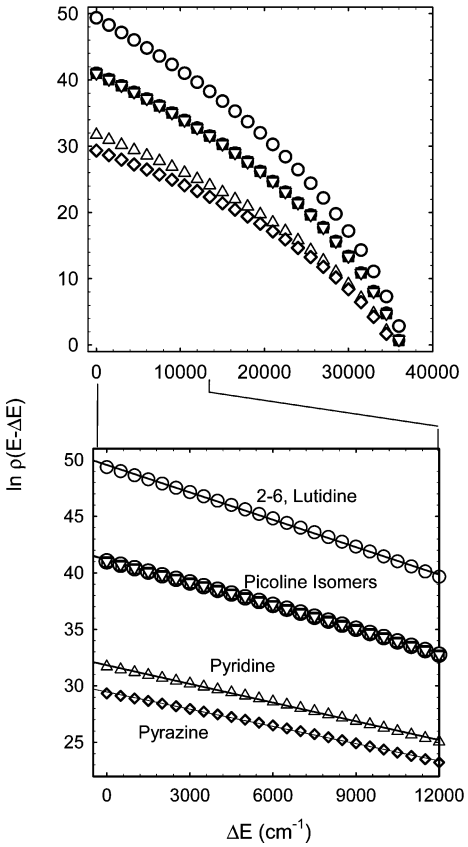

Figure 9. Semilog plots of the donor vibrational state density as a function of internal energy. The state density for each donor was fit to an exponential decay in energy with a fitting parameter β_ρ.

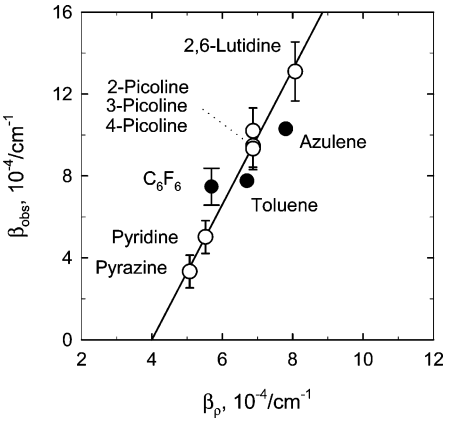

Figure 10. Correlation of the experimentally determined β_{obs} values with calculated β_ρ values for quenching of highly vibrationally excited azabenzenes with CO_2. A similar correlation has also been observed for quenching in H_2O (refs 31 and 32).

10. The similarity in the quenching behavior for the picoline isomers is also evident in Figure 10.

To test further the correlation of $P(\Delta E)$ with the donor state density, we compare the state density and collisional relaxation profiles of three other molecules for which the high energy part of $P(\Delta E)$ has been measured in collisions with CO_2. The relaxation of highly excited hexafluorobenzene[38] has been measured using diode laser probing and azulene[8] and toluene[6] have been measured using KCSI. The β_{obs} parameters for these molecules are derived from fitting constants reported in the original publications. The β_ρ parameters are determined from state density calculations based on harmonic frequencies. The results are included in Table 3 and in Figure 10 as filled circles. The data for these molecules correlates fairly well with their state density and provides additional evidence that the shape of the high energy part of the energy transfer distribution function for these molecules can be predicted from the energy dependence of the state density.

It is somewhat surprising that such a clear correlation is observed between the distribution function for impulsive energy transfer and the total state density. In impulsive collisions of highly vibrationally excited polyatomic molecules, one does not expect the entire phase space to be explored. Instead, one might expect the local state density at the area of impact to be responsible for the energy transfer. There is evidence, however, from a number of classical trajectory simulations that chattering collisions are not uncommon when highly vibrationally excited molecules undergo quenching with small molecular collision partners.[7,22,24,25,30,39] Chattering collisions involve multiple sequential points of contact between the collision partners during which energy is transferred via a number of impulsive encounters. Chattering collisions are observed for both small and large ΔE values. It is possible that such a mechanism promotes the anharmonic coupling that enhances intramolecular vibrational relaxation in highly excited donor molecules. It would be interesting to see if the correlation breaks down when the donor molecule has distinct regions of high and low state density. In this case, it is possible that the energy transfer distribution function will correlate with a subset of local oscillators and show deviations from the linear correlation in Figure 10.

The correlation shown in Figure 10 is consistent with predictions of the GRETCHEN model, which says that the shape of the distribution function should have essentially the same energy dependence as the state density.[31−33] Of course, the observed correlation may also be consistent with other statistical approaches such as those presented by Rabinovitch,[10] Troe,[13,14] and Nordholm[15] and their co-workers. It would be interesting to compare our results with other models of energy transfer involving relatively large, highly vibrationally excited molecules.

Conclusions

The collisional relaxation of highly vibrationally excited 3- and 4-picoline with CO_2 has been investigated using transient IR probing of energy gain in CO_2 and compared to earlier results for the quenching of 2-picoline with CO_2. The energy transfer profiles for impulsive collisions with $\Delta E > 3000$ cm^{-1} are nearly identical for all three isomers. The shapes of the large ΔE energy transfer distribution functions for the picoline donors are very similar to one another. In addition, the observed high energy tail of the distribution functions correlate with total state density of the vibrationally hot molecule. This work highlights the statistical nature of collisional quenching in highly excited molecules even when there is clear evidence that the relaxation occurs via impulsive collisions. These studies provide further support that state density may be an important predictive tool in modeling the chemistry of high temperature and high energy environments. Future studies will investigate a broader range of donor molecules with a variety of functional groups, structures and degrees of floppiness to ascertain how broadly total state density is a good descriptor of the high energy tail of the energy transfer distribution function for highly vibrationally excited molecules. In addition, transient IR probe techniques will be applied to a broader range of collision partners to include a larger range of bath properties such as polarity, mass and moment of inertia. Energy gain studies on DCl have recently been reported[40] and new studies are underway on energy gain in CH_4 and NH_3.

Acknowledgment. The authors thank Dr. Ziman Li for scientific contributions throughout this project. E.M.M. was a Beckman Scholar (2003−2005) supported by the Arnold and Mabel Beckman Foundation. E.M.M., N.B., and M.H. received support from the Boston University Undergraduate Research Opportunities Program. A.S.M. was a Camille Dreyfus Teacher-Scholar (1995−2004) and received support from the Camille and Henry Dreyfus Foundation. These studies were funded by the Department of Energy (DE-FG02-03ER15429) with additional equipment support from the National Science Foundation (CHE-0316836).

References and Notes

(1) Baer, T.; Hase, W. L. *Unimolecular Reaction Dynamics. Theory and Experiments*; Oxford University Press: New York, 1996.
(2) Mullin, A. S.; Park, J.; Chou, J. Z.; Flynn, G. W.; Weston, R. E. *Chem. Phys.* **1993**, *175*, 53.
(3) Michaels, C. A.; Mullin, A. S.; Flynn, G. W. *J. Chem. Phys.* **1995**, *102*, 6682.
(4) Mullin, A. S.; Michaels, C. A.; Flynn, G. W. *J. Chem. Phys.* **1995**, *102*, 6032.
(5) Hold, U.; Lenzer, T.; Luther, K.; Reihs, K.; Symonds, A. C. *J. Chem. Phys.* **2000**, *112*, 4076.
(6) Lenzer, T.; Luther, K.; Reihs, K.; Symonds, A. C. *J. Chem. Phys.* **2000**, *112*, 4090.
(7) Grigoleit, U.; Lenzer, T.; Luther, K.; Mützel, M.; Takahara, A. *Phys. Chem. Chem. Phys.* **2001**, *3*, 2191.
(8) Hold, U.; Lenzer, T.; Luther, K.; Symonds, A. C. *J. Chem. Phys.* **2003**, *119*, 11192.
(9) Gilbert, R. G. *J. Chem. Phys.* **1984**, *80*, 5501.
(10) Tardy, D. C.; Rabinovitch, B. S.; Larson, C. W. *J. Chem. Phys.* **1966**, *45*, 1163.
(11) Lin, Y. N.; Rabinovitch, B. S. *J. Phys. Chem.* **1970**, *74*, 3151.
(12) Troe, J. *Ber. Bunsen-Ges. Phys. Chem.* **1973**, *77*, 665.
(13) Troe, J. *J. Chem. Phys.* **1977**, *66*, 4758.
(14) Hippler, H.; Troe, J. In *Bimolecular Reactions*; Baggot, J. E., Ashfold, M. N. R., Eds.; The Royal Chemical Society: London, 1989.
(15) Nilsson, D.; Nordholm, S. *J. Chem. Phys.* **2002**, *116*, 7040.
(16) Lim, K. F.; Gilbert, R. G. *J. Chem. Phys.* **1990**, *92*, 1819.
(17) Lenzer, T.; Luther, K.; Troe, J.; Gilbert, R. G.; Lim, K. F. *J. Chem. Phys.* **1995**, *103*, 626.
(18) Lenzer, T.; Luther, K. *J. Chem. Phys.* **1996**, *105*, 10944.
(19) Lenzer, T.; Luther, K. *J. Chem. Phys.* **1996**, *104*, 3391.
(20) Lenzer, T.; Luther, K. *Ber. Bunsen-Ges. Phys. Chem.* **1997**, *101*, 581.
(21) Grigoleit, U.; Lenzer, T.; Luther, K. *Z. Phys. Chem. (Munich)* **2000**, *214*, 1065.
(22) Linhananta, A.; Lim, K. G. *Phys. Chem. Chem. Phys.* **2002**, *4*, 577.
(23) Oref, I. *Chem. Phys.* **1994**, *187*, 163.
(24) Bernshtein, V.; Oref, I. *J. Phys. Chem. B* **2005**, *109*, 8310.
(25) Bernshtein, V.; Oref, I. *J. Phys. Chem. A* **2001**, *105*, 10646.
(26) Bernshtein, V.; Oref, I. *J. Chem. Phys.* **1998**, *108*, 3543.
(27) Bernshtein, V.; Oref, I.; Lendvay, G. *J. Phys. Chem. A* **1997**, *101*, 2445.
(28) Higgins, C.; Ju, Q.; Seiser, N.; Flynn, G. W.; Chapman, S. *J. Phys. Chem. A* **2001**, *105*, 2858.
(29) Higgins, C. J.; Chapman, S. *J. Phys. Chem. A* **2004**, *108*, 8009.
(30) Li, Z.; Sansom, R.; Bonella, S.; Coker, D.; Mullin, A. *J. Phys. Chem. A* **2005**, *109*, 7658.
(31) Elioff, M. S.; Fang, M.; Mullin, A. S. *J. Chem. Phys.* **2001**, *115*, 6990.
(32) Elioff, M. S.; Fang, M.; Mullin, A. S. *J. Chem. Phys.* **2002**, *117*, 6880.
(33) Park, J.; Shum, L.; Lemoff, A. S.; Werner, K.; Mullin, A. S. *J. Chem. Phys.* **2002**, *117*, 5221.
(34) Wall, M. C.; Stewart, B. A.; Mullin, A. S. *J. Chem. Phys.* **1998**, *108*, 6185.
(35) Rothman, L. S. R.; C. P.; Goldman, A.; Massie, S. T.; Edwards, D. P.; Flaud, J.-M.; Perrin, A.; Camy-Peyret, C.; Dana, V.; Mandin, J.-Y.; Schroeder, J.; McCann, A.; Gamache, R. R.; Wattson, R. B.; Yoshino, K.; Chance, K. V.; Jucks, K. W.; Brown, L. R.; Nemtchinov, V.; Varanasi, P. *J. Quantum Spec. Rad. Trans.* **1998**, *60*, 665.
(36) Michaels, C. A.; Flynn, G. W. *J. Chem. Phys.* **1997**, *106*, 3558.
(37) Beyer, T.; Swinehart, D. R. *ACM Commun.* **1973**, *16*.
(38) Michaels, C. A.; Lin, Z.; Mullin, A. S.; Tapalian, H. C.; Flynn, G. W. *J. Chem. Phys.* **1997**, *106*, 7055.
(39) Clarke, D. L.; Oref, I.; Gilbert, R. G.; Lim, K. G. *J. Chem. Phys.* **1992**, *96*, 5983.
(40) Li, Z.; Korobkova, E.; Werner, K.; Shum, L.; Mullin, A. S. *J. Chem. Phys.* **2005**, *123*, 174306.